the neutral B anomalies, the 6d global fit and new visualisation tools

German Valencia

based on:
Bernat Capdevila, Ursula Laa, G. V. EPJC (2019)
arXiv:1811.10793
and work in progress

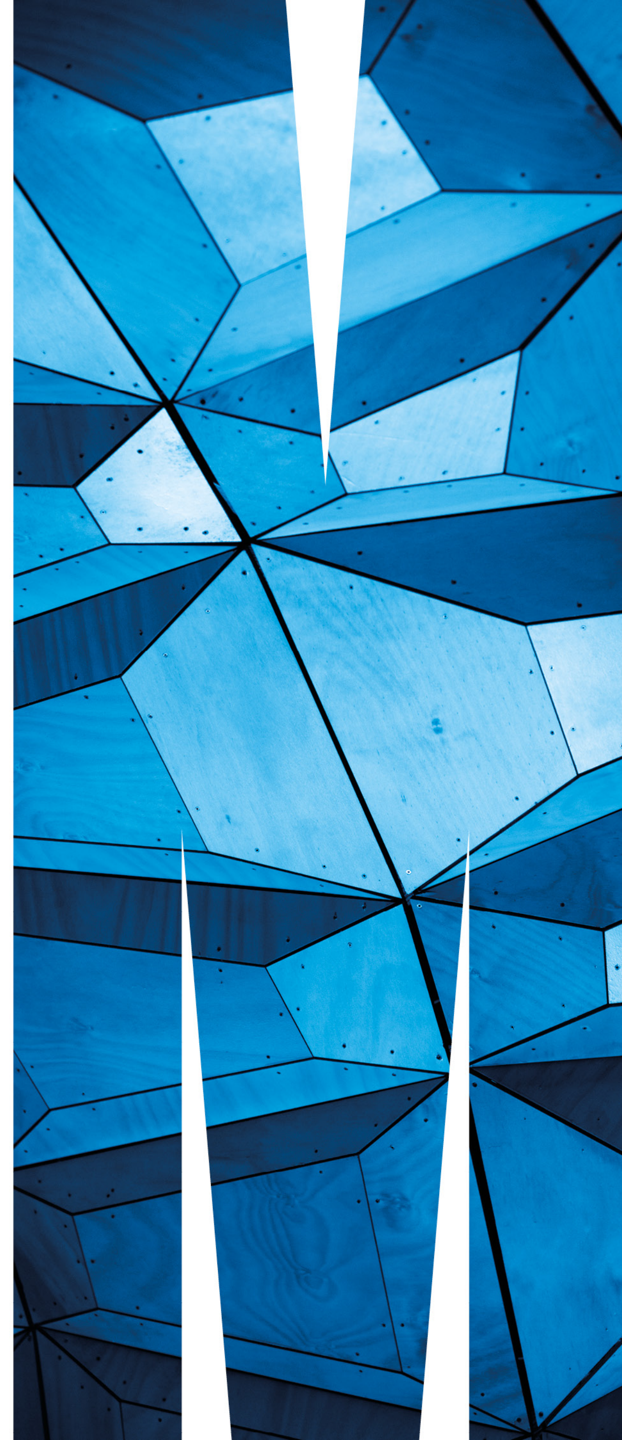

the neutral current B anomalies

- detailed measurements of processes with a quark level transition $b \to s\, \mu^+ \mu^-$ (and also some $b \to s\, e^+ e^-$)
- small problems showing up since around 2009, none particularly exciting by itself
- cumulative effect appears to go against the SM with claims of $> 5\sigma$ significance
- three aspects: the global fit (this talk), new physics, matrix elements
- best hints for LFUV are the ratios R_K and R_{K^*}
- more subtle deviations in details of angular distributions and branching ratios

New Physics?

LHCb collaboration, Phys. Rev. Lett. 113 (2014) 151601

after Moriond 2019

2.5σ

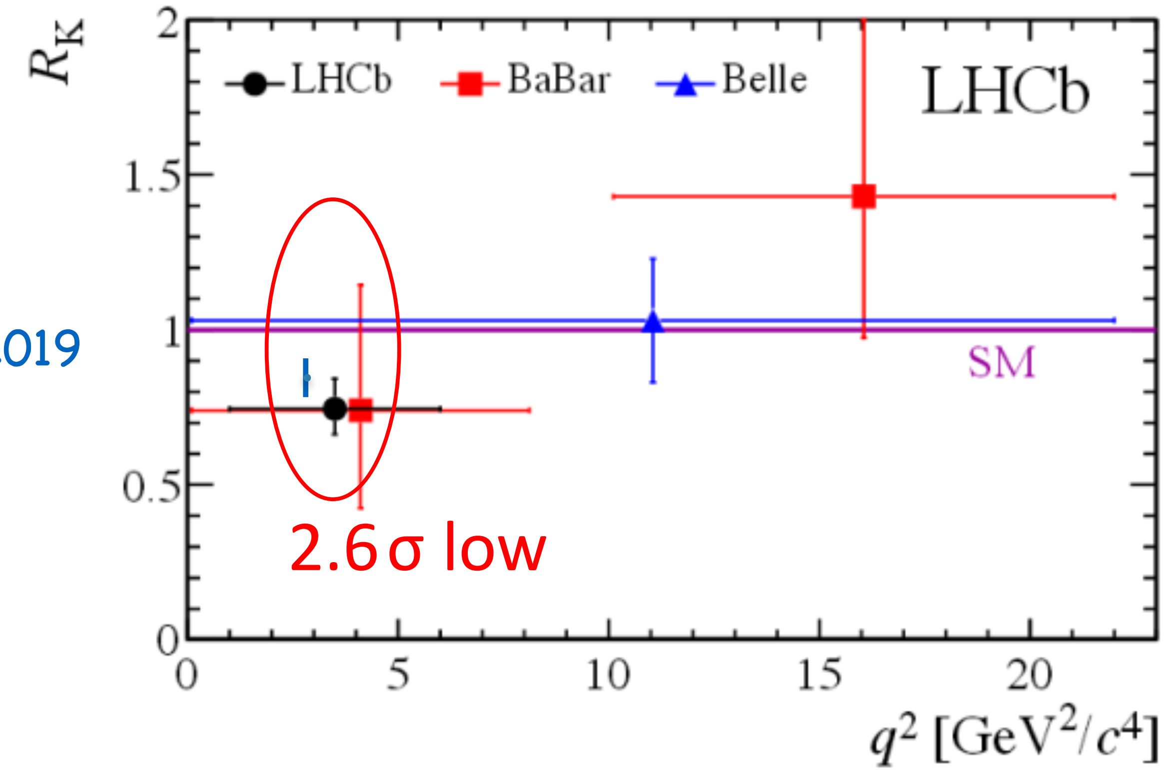

PRL 113 (2014) 151601

$$R_K = \frac{\mathrm{BR}(B \to K\mu^+\mu^-)}{\mathrm{BR}(B \to Ke^+e^-)} = 0.745^{+0.090}_{-0.074} \pm 0.036$$

vs 1.00 ± 0.01 in SM

$$R_K^{[1.1,6]} = \frac{\mathcal{B}(B \to K\mu^+\mu^-)}{\mathcal{B}(B \to Ke^+e^-)} = 0.846^{+0.060}_{-0.054}{}^{+0.016}_{-0.014}$$

LHCb arXiv:1903.09252 [hep-ex].

the less obvious NP case

- Most prominent deviation in $B^0 \to K^{0*}\mu^+\mu^-$ is in the angular distribution of the muons for the low di-muon invariant mass region through "P'_5"

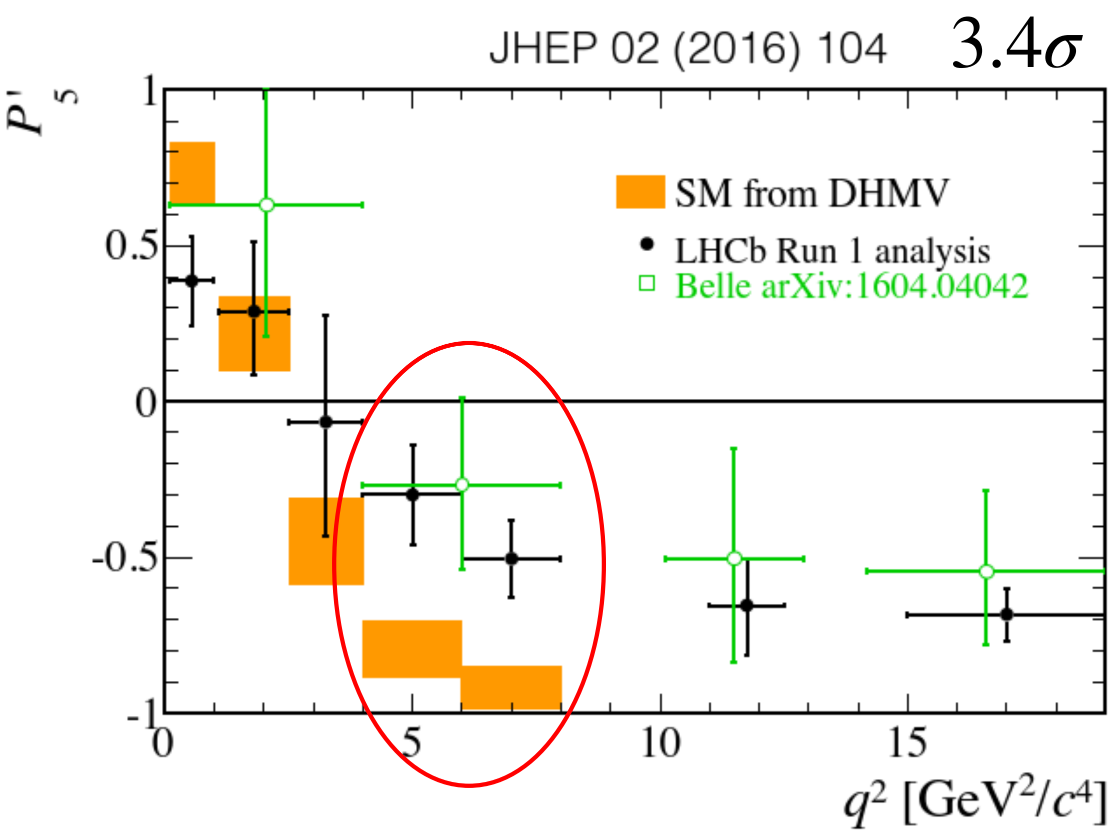

The 6d global fit

- our starting point is S. Descotes-Genon, et.al. JHEP 06 (2016) 092

$$\mathcal{O}_7 = \frac{e}{16\pi^2} m_b (\bar{s}\sigma_{\mu\nu} P_R b) F^{\mu\nu},$$
$$\mathcal{O}_9 = \frac{e^2}{16\pi^2} (\bar{s}\gamma_\mu P_L b)(\bar{\ell}\gamma^\mu \ell),$$
$$\mathcal{O}_{10} = \frac{e^2}{16\pi^2} (\bar{s}\gamma_\mu P_L b)(\bar{\ell}\gamma^\mu \gamma_5 \ell),$$

$$\mathcal{O}_{7'} = \frac{e}{16\pi^2} m_b (\bar{s}\sigma_{\mu\nu} P_L b) F^{\mu\nu},$$
$$\mathcal{O}_{9'} = \frac{e^2}{16\pi^2} (\bar{s}\gamma_\mu P_R b)(\bar{\ell}\gamma^\mu \ell),$$
$$\mathcal{O}_{10'} = \frac{e^2}{16\pi^2} (\bar{s}\gamma_\mu P_R b)(\bar{\ell}\gamma^\mu \gamma_5 \ell),$$

$$\mathcal{H}_{\text{eff}} = -\frac{4G_F}{\sqrt{2}} V_{tb} V_{ts}^* \sum_i \mathcal{C}_i O_i$$

$$C_i = C_i^{SM} + C_i^{NP}$$

$$C_{7,9,10}^{SM} = -0.29,\ 4.07,\ -4.31$$

float $C_7^{NP}, C_{7'}^{NP}, C_{9\mu}^{NP}, C_{9'\mu}^{NP}, C_{10\mu}^{NP}, C_{10'\mu}^{NP}$

Best fit (BF) parameters obtained by minimising

$$\chi^2(\mathcal{C}_k) = \sum_{i,j=1}^{N_{\text{obs}}} \left[O_i^{\text{exp}} - O_i^{\text{th}}(\mathcal{C}_k)\right] (C_{\text{exp}} + C_{\text{th}})_{ij}^{-1} \left[O_j^{\text{exp}} - O_j^{\text{th}}(\mathcal{C}_k)\right]$$

the observables

- include 175 observables
- branching ratios and parameters in the angular distributions in different bins of dilepton invariant mass
- processes:
  - $B^{(0,+)} \to K^{*(0,+)}\mu^+\mu^-$, $B^{(0,+)} \to K^{*(0,+)}e^+e^-$, $B^{(0,+)} \to K^{*(0,+)}\gamma$,
  - $B^{(0,+)} \to K^{(0,+)}\mu^+\mu^-$, $B^+ \to K^+e^+e^-$ (through the R_K observable),
  - $B_s \to \phi\mu^+\mu^-$, $B_s \to \phi\gamma$,
  - $B \to X_s\mu^+\mu^-$, $B \to X_s\gamma$ and $B_s \to \mu^+\mu^-$.
- from Belle, LHCb, Atlas, CMS and HFLAV combinations

P_5': the angular distribution

optimised observables
Descotes-Genon et al,
JHEP 05 (2013) 137

$$P'_{i=4,5,6,8} = \frac{S_{j=4,5,7,8}}{\sqrt{F_{\mathrm{L}}(1-F_{\mathrm{L}})}}$$

$$P_{1,2,3} = \frac{2S_3, -1/2S_6, -S_9}{(1-F_L)}$$

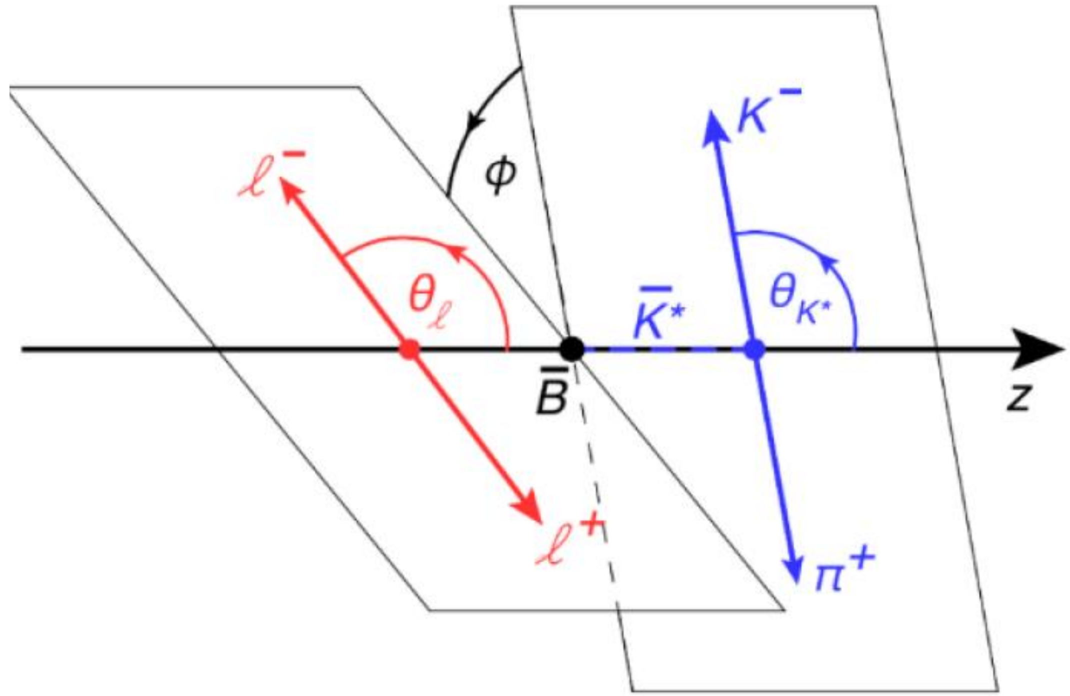

$$\frac{1}{\mathrm{d}\Gamma/dq^2}\frac{\mathrm{d}^4\Gamma}{\mathrm{d}\cos\theta_\ell\,\mathrm{d}\cos\theta_K\,\mathrm{d}\phi\,\mathrm{d}q^2} = \frac{9}{32\pi}\Big[\frac{3}{4}(1-F_{\mathrm{L}})\sin^2\theta_K + F_{\mathrm{L}}\cos^2\theta_K + \frac{1}{4}(1-F_{\mathrm{L}})\sin^2\theta_K\cos 2\theta_\ell$$
$$- F_{\mathrm{L}}\cos^2\theta_K\cos 2\theta_\ell + S_3\sin^2\theta_K\sin^2\theta_\ell\cos 2\phi$$
$$+ S_4\sin 2\theta_K\sin 2\theta_\ell\cos\phi + S_5\sin 2\theta_K\sin\theta_\ell\cos\phi$$
$$+ S_6\sin^2\theta_K\cos\theta_\ell + S_7\sin 2\theta_K\sin\theta_\ell\sin\phi$$
$$+ S_8\sin 2\theta_K\sin 2\theta_\ell\sin\phi + S_9\sin^2\theta_K\sin^2\theta_\ell\sin 2\phi\Big]$$

Correlation Map: some correlations are known

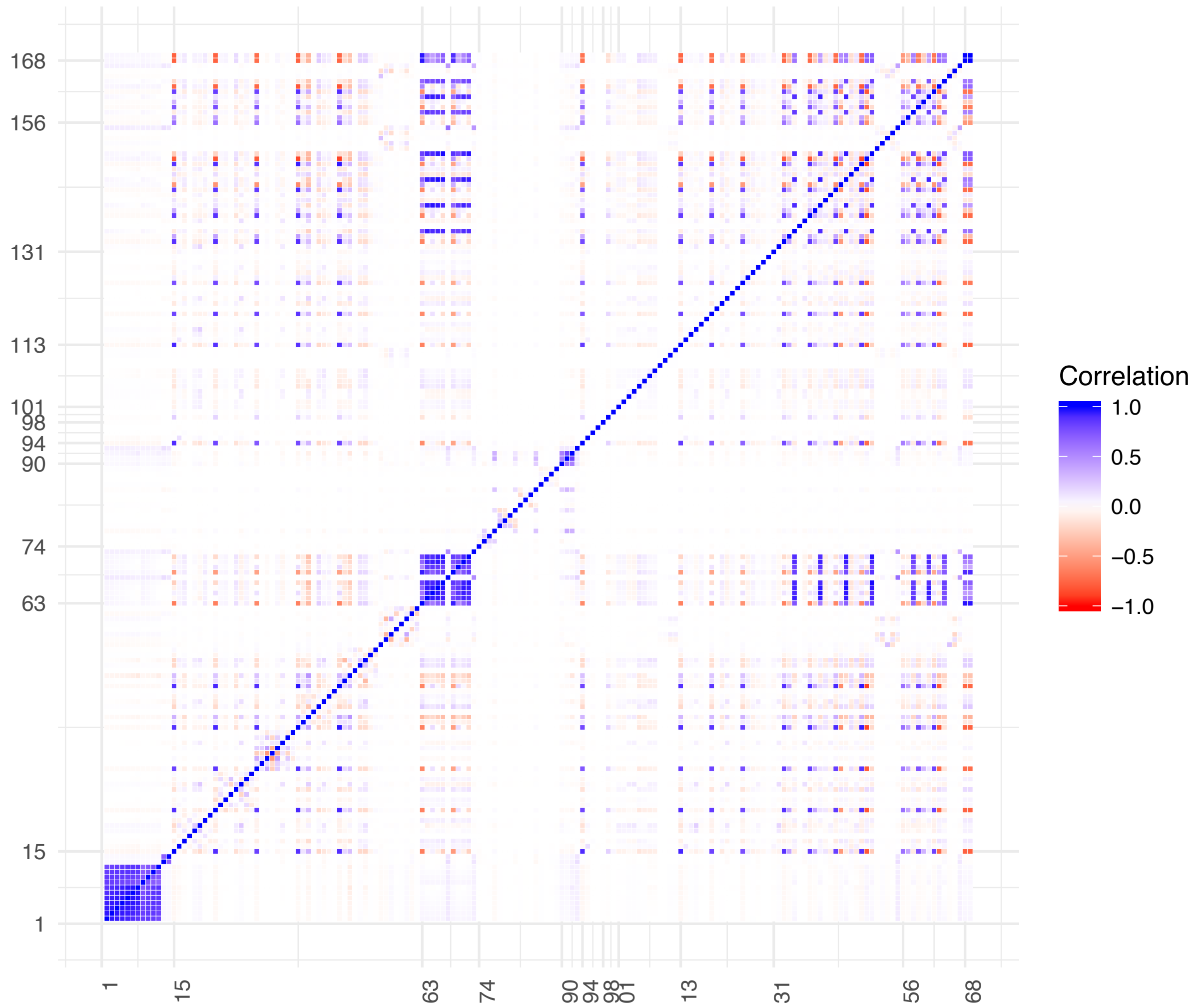

Previous Results

Tabulated results from B. Capdevila et. al. JHEP 01 (2018) 093

1-d

	All			
1D Hyp.	Best fit	1 σ	2 σ	$\mathrm{Pull}_{\mathrm{SM}}$
$\mathcal{C}_{9\mu}^{\mathrm{NP}}$	-1.11	$[-1.28, -0.94]$	$[-1.45, -0.75]$	5.8
$\mathcal{C}_{9\mu}^{\mathrm{NP}} = -\mathcal{C}_{10\mu}^{\mathrm{NP}}$	-0.62	$[-0.75, -0.49]$	$[-0.88, -0.37]$	5.3
$\mathcal{C}_{9\mu}^{\mathrm{NP}} = -\mathcal{C}'_{9\mu}$	-1.01	$[-1.18, -0.84]$	$[-1.34, -0.65]$	5.4

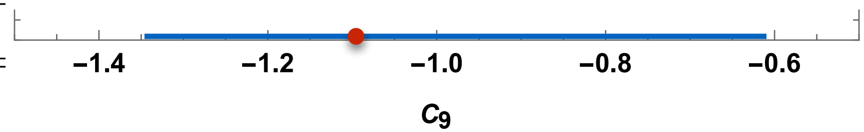

1-d fit can quantify uncertainty in parameter space

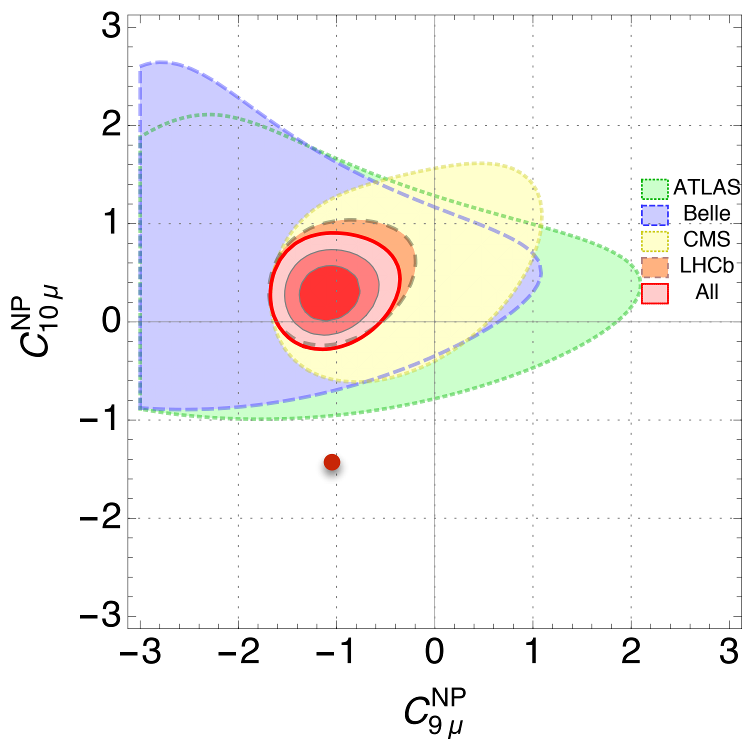

2d fits show correlations between parameters

for 1d results, show projections or slices? where?

six parameter fit - 6d picture

	$\mathcal{C}_7^{\mathrm{NP}}$	$\mathcal{C}_{9\mu}^{\mathrm{NP}}$	$\mathcal{C}_{10\mu}^{\mathrm{NP}}$	$\mathcal{C}_{7'}$	$\mathcal{C}_{9'\mu}$	$\mathcal{C}_{10'\mu}$
Best fit	+0.03	-1.12	+0.31	+0.03	+0.38	+0.02
1 σ	$[-0.01, +0.05]$	$[-1.34, -0.88]$	$[+0.10, +0.57]$	$[+0.00, +0.06]$	$[-0.17, +1.04]$	$[-0.28, +0.36]$
2 σ	$[-0.03, +0.07]$	$[-1.54, -0.63]$	$[-0.08, +0.84]$	$[-0.02, +0.08]$	$[-0.59, +1.58]$	$[-0.54, +0.68]$

- Characterisation beyond just the best fit (BF) point
- meaning of 1σ ranges?
- How does the 6d fit differ from lower dimensional ones
- Which observables are important in constraining the parameters
- Fit in observable space and role of correlation
- Predictions in the context of the fit rather than for the BF only

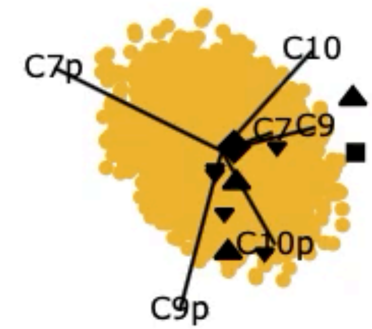

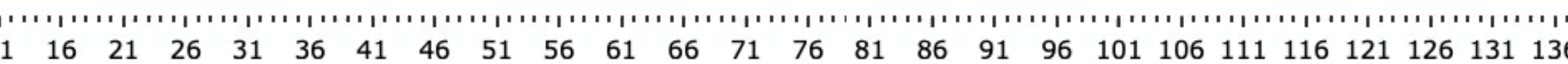

Visualising the 6d 1 sigma region relative to BF, lower dimensional best fits and the SM

PPI maximising distance to SM produces the projection shown before

visualisation of 1 sigma region

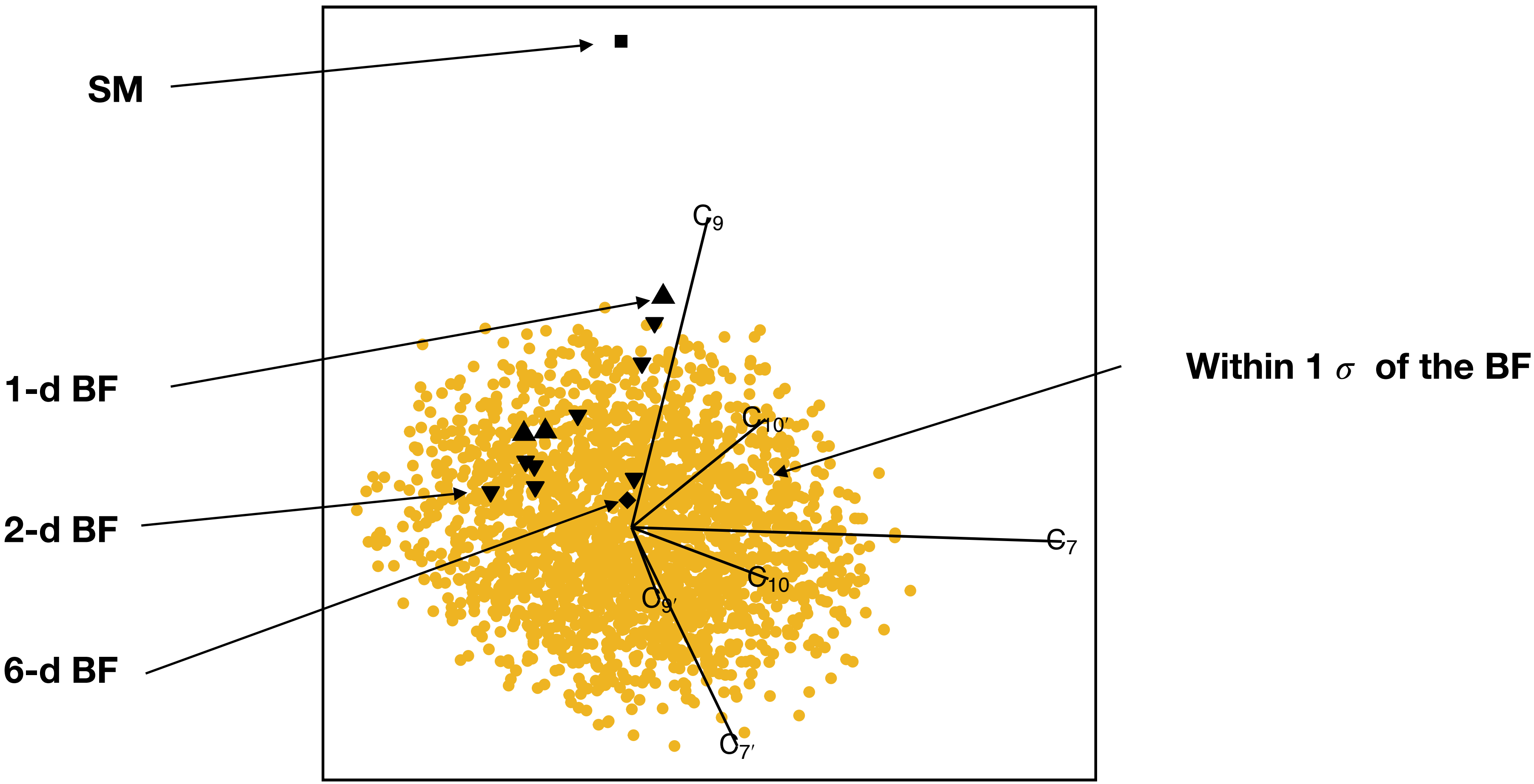

- axes centred with respect to point cloud, not at BF
- directions are centred and scaled

data vs SM and vs BF:

$$\mathrm{Pull}(p) = \frac{T(p) - \mathcal{O}}{\sqrt{\Delta^2_{exp} + \Delta^2_{T(p)}}}$$

SM

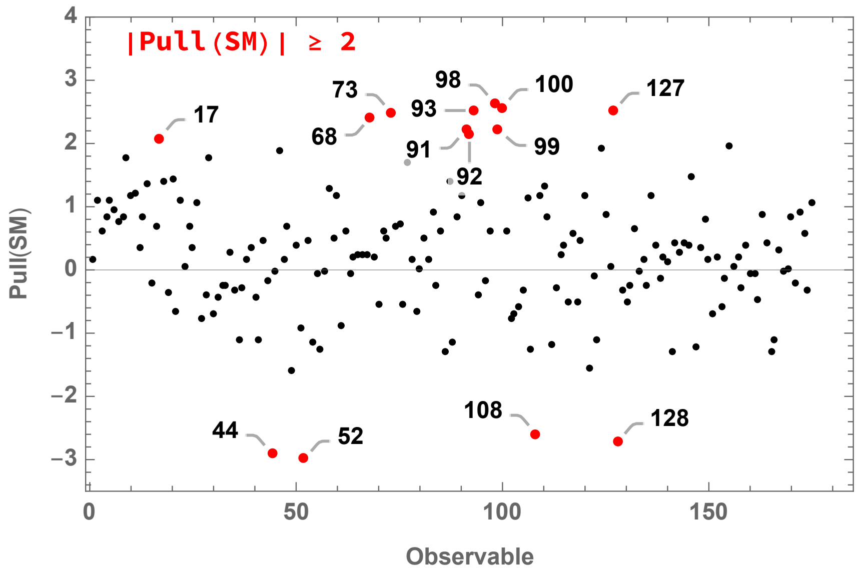

BF

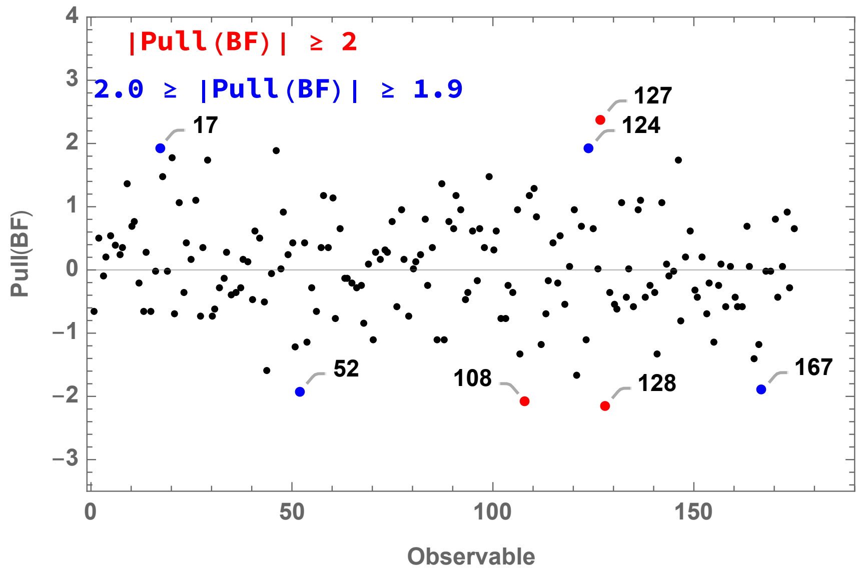

44	$P_5'(B \to K^* \mu\mu)[4-6]$
52	$P_5'(B \to K^* \mu\mu)[6-8]$

98	$R_K(B^+ \to K^+)[1-6]$
99	$R_{K^*}(B^0 \to K^{0*})[0.045-1.1]$
100	$R_{K^*}(B^0 \to K^{0*})[1.1-6]$

52 stands out against both the SM and the BF

no so 44, 98, 99, 100

Pull Differences and Correlation

$$\mathrm{Pull}_\sigma(p) = \sum_j \sigma_{ij}^{-1/2}(T(p)-O)_j$$

include correlated uncertainties

$$\Delta(\mathrm{Pull}) \; = \; |\mathrm{Pull(SM)}| - |\mathrm{Pull(BF)}|$$

>0 implies better agreement with BF

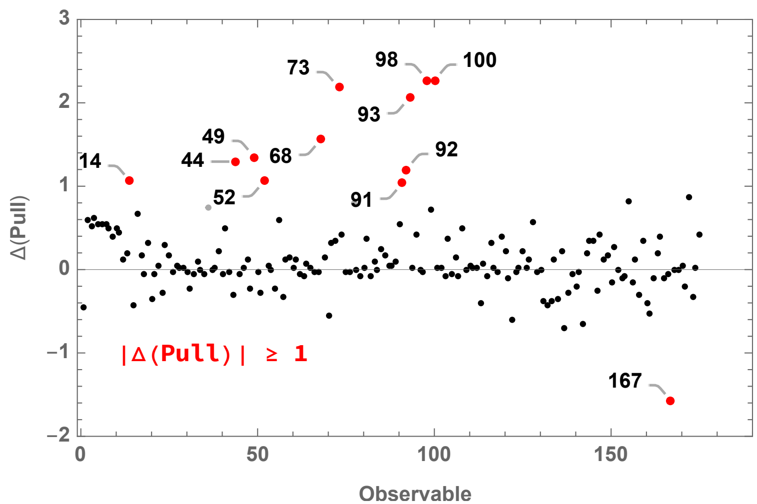

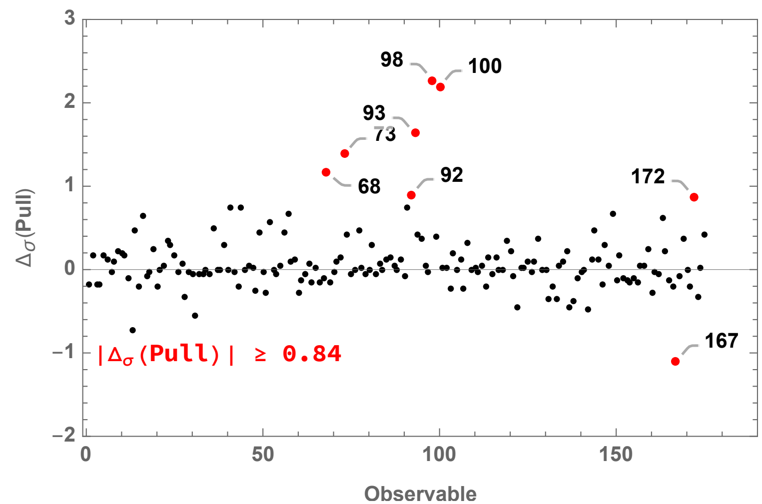

44	$P_5'(B \to K^*\mu\mu)[4-6]$	98	$R_K(B^+ \to K^+)[1-6]$	$LHCb$
52	$P_5'(B \to K^*\mu\mu)[6-8]$	100	$R_{K^*}(B^0 \to K^{0*})[1.1-6]$	$LHCb$

correlations reduce the significance of some angular observables, like P_5' (44, 52) which appear in the left but not the right plot.
This is in contrast to R_K, R_{K^*} (98, 100)

predictions in context of the fit

- the χ^2 function is only known numerically for a discrete set of points
- use Hessian matrix to approximate the χ^2 function near the global minimum

$$\chi^2 = \chi_0^2 + \sum_{i,j} H_{ij}\, y_i\, y_j\,,$$

$$H_{ij} = \frac{1}{2}\left(\frac{\partial^2 \chi^2}{\partial y_i\, \partial y_j}\right)_0\,,$$

$$y_i = a_i - a_i^0$$

fit parameter **value at the minimum**

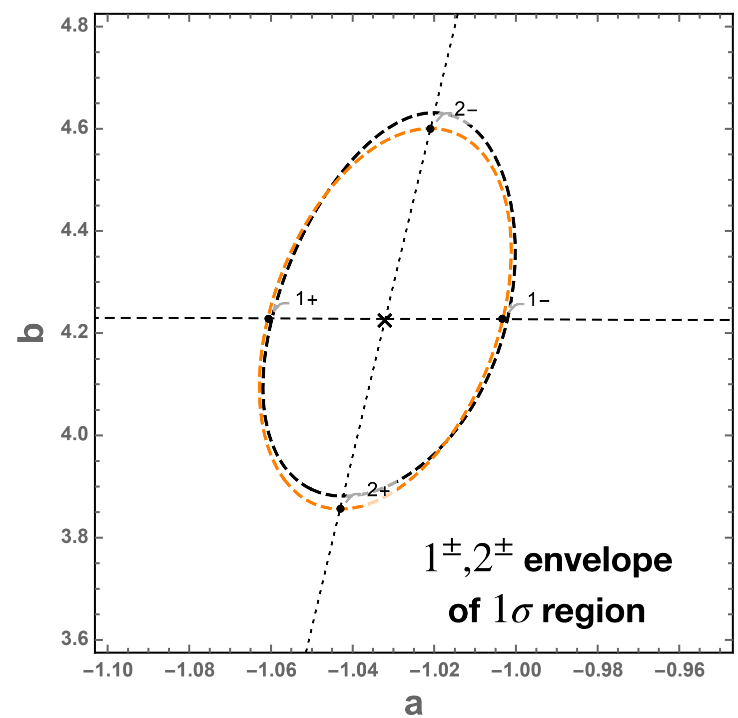

- Eigenvectors are principal axes of the approximate confidence level ellipsoids
- Eigenvalues encode how tightly each direction is constrained by the data

lower dimensional fits from the Hessian

- very quickly produce any lower dimensional fit
- i.e.: after Moriond BF fit has a reduced $\Delta\chi^2$ from the SM implied change of $< 0.1\ \sigma$
- 2d projections or slices of 6d 1σ cloud
- fast test of NP scenarios

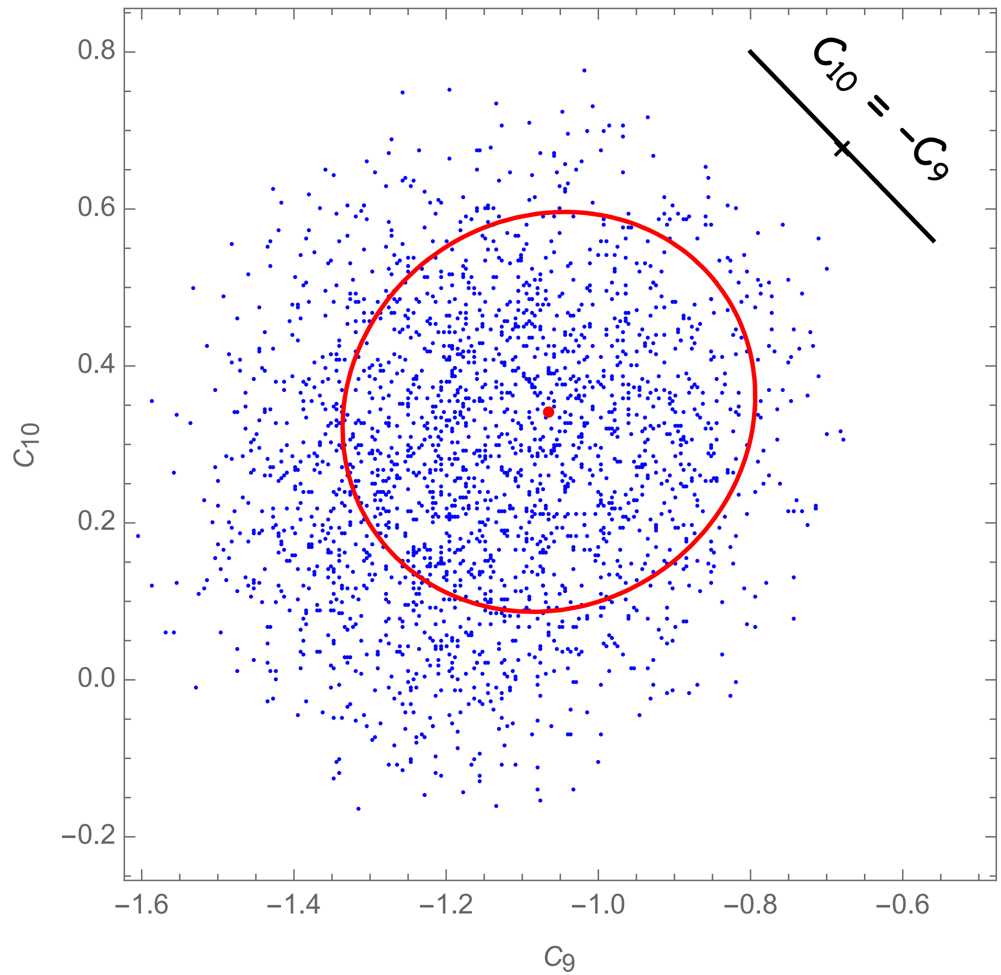

Normalised eigenvectors

eigenvalues: HD =diag(6621,5647,115.6,72.6,44.7, 6.1)

eigenvector	C_7	C_9	C_{10}	$C_{7'}$	$C_{9'}$	$C_{10'}$
1	0.996	0.0317	-0.000796	-0.0841	0.00334	-0.00924
2	-0.0836	-0.01	-0.00843	-0.996	-0.0114	0.0181
3	0.0192	-0.267	-0.306	0.023	-0.361	0.839
4	0.0169	-0.466	0.859	-0.000316	-0.192	0.0824
5	0.023	-0.843	-0.374	0.0015	0.243	-0.3
6	0.000335	0.0212	0.166	-0.0036	0.88	0.445

- large alignment with one WC only for 1^{+-} directions. These are the most constrained (largest eigenvalues), corresponding closely to the parameters C_7, $C_{7'}$ respectively
- PCA: in this case all six directions are important, explaining between 31% to 13% of the variance in the data

visualising projections

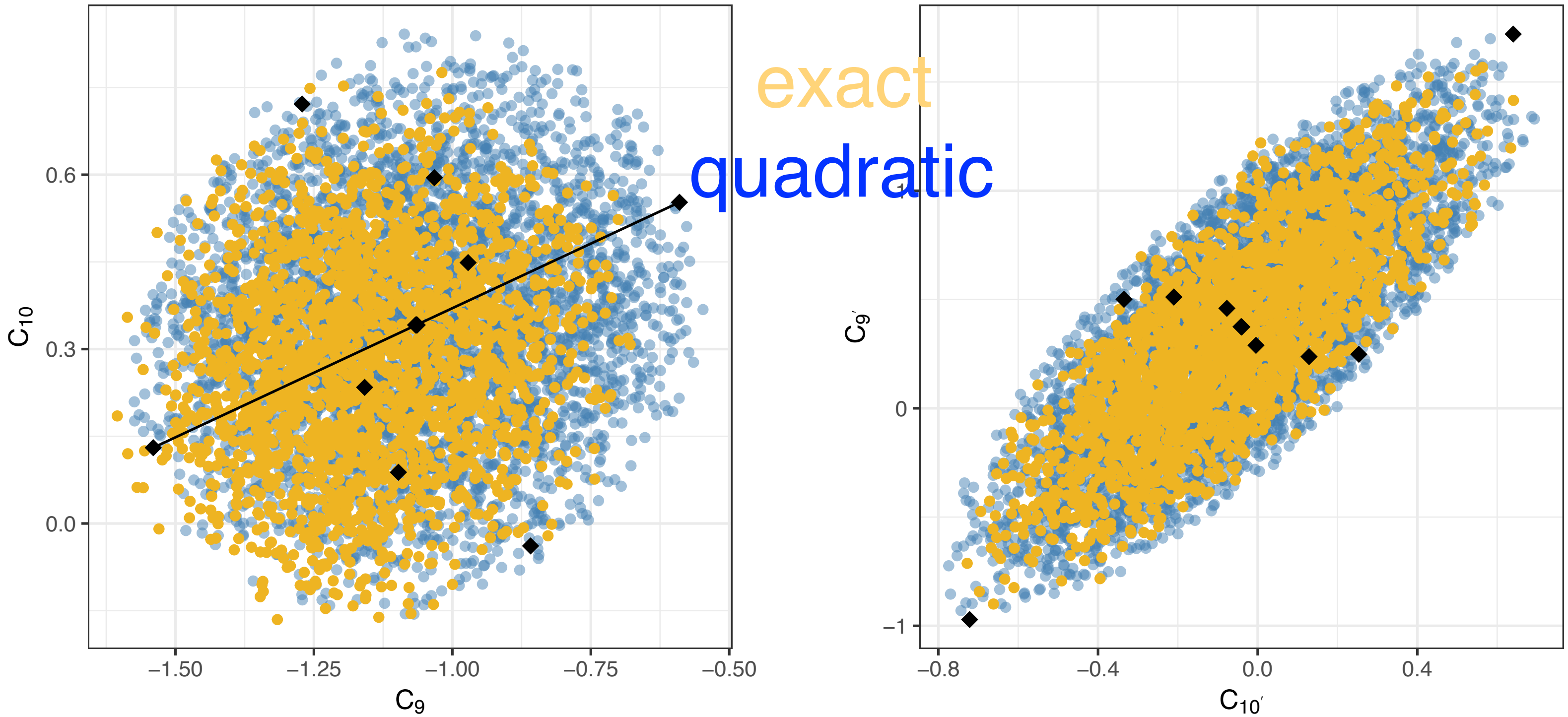

- 12 SVD point envelope shown in two projections
- line in the left plot shows direction 5 (mostly along C_9): the Hessian approximation does not capture the asymmetric shape in this case
- right plot reveals a strong correlation between $C_{9'}$ and $C_{10'}$
- right plot illustrates the importance of the SVD envelope

Fit Uncertainty

- Use the SVD points to evaluate fit uncertainty (6d or maximum)
- can also visualise as 6d uncertainty

Measured
SM prediction
BF prediction
Fit uncertainty

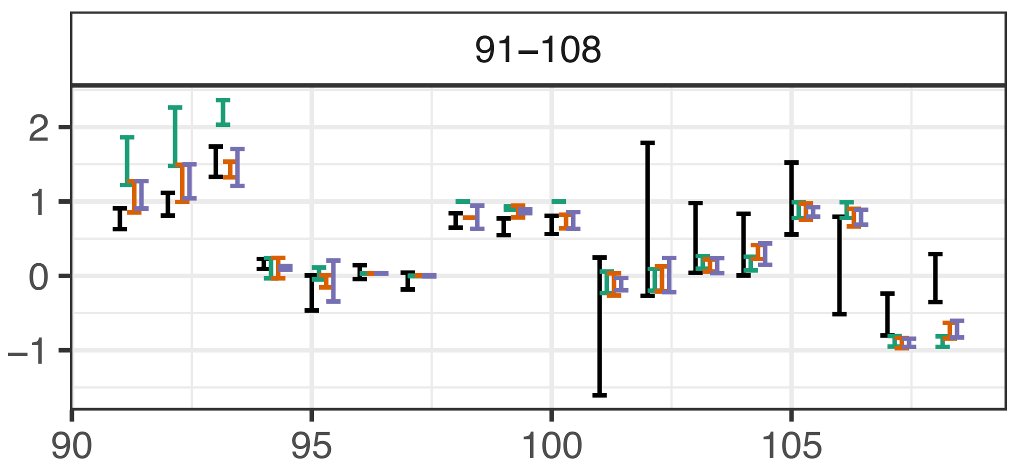

ID	Observable	Exp
91	$10^7 \times Br(B_s \to \Phi\mu\mu)[2-5]$	LHCb [26]
92	$10^7 \times Br(B_s \to \Phi\mu\mu)[5-8]$	LHCb [26]
93	$10^7 \times Br(B_s \to \Phi\mu\mu)[15-18.8]$	LHCb [26]
94	$F_L(B \to K^*ee)[0.0020-1.120]$	LHCb [27]
95	$P_1(B \to K^*ee)[0.0020-1.120]$	LHCb [27]
96	$P_2(B \to K^*ee)[0.0020-1.120]$	LHCb [27]
97	$P_3(B \to K^*ee)[0.0020-1.120]$	LHCb [27]
98	$R_K(B^+ \to K^+)[1-6]$	LHCb [28]
99	$R_{K^*}(B^0 \to K^{0*})[0.045-1.1]$	LHCb [29]
100	$R_{K^*}(B^0 \to K^{0*})[1.1-6]$	LHCb [29]
101	$P_4'(B \to K^*ee)[0.1-4]$	Belle [30]
102	$P_4'(B \to K^*\mu\mu)[0.1-4]$	Belle [30]
103	$P_5'(B \to K^*ee)[0.1-4]$	Belle [30]
104	$P_5'(B \to K^*\mu\mu)[0.1-4]$	Belle [30]
105	$P_4'(B \to K^*ee)[4-8]$	Belle [30]
106	$P_4'(B \to K^*\mu\mu)[4-8]$	Belle [30]
107	$P_5'(B \to K^*ee)[4-8]$	Belle [30]
108	$P_5'(B \to K^*\mu\mu)[4-8]$	Belle [30]

large $\Delta\chi^2 \longleftrightarrow$ error << fit uncertainty, important observable

Relating Observables and Parameter Directions

Change in predicted value when moving 1σ in SVD a given direction, normalised to the error

$$\delta_i = \frac{(T_i - T_{BF})}{\sqrt{\Delta^2_{exp} + \Delta^2_{BF}}}$$

Taking into account correlated errors

$$\delta_{\sigma,i} = \sum_l \sigma_{il}^{-1/2} (T_{pt} - T_{BF})_l$$

- ❓ Which observables change most in each direction
- ❓ Which directions result in the largest variation in predictions
- ❓ How important are correlation effects

Ranking Observables

Without correlation

Mostly C_7

1+		1-	
ID	δ^2	ID	δ^2
171	4.07	171	5.03
170	0.58	170	0.74
41	0.56	41	0.52
90	0.34	90	0.46
49	0.31	49	0.39

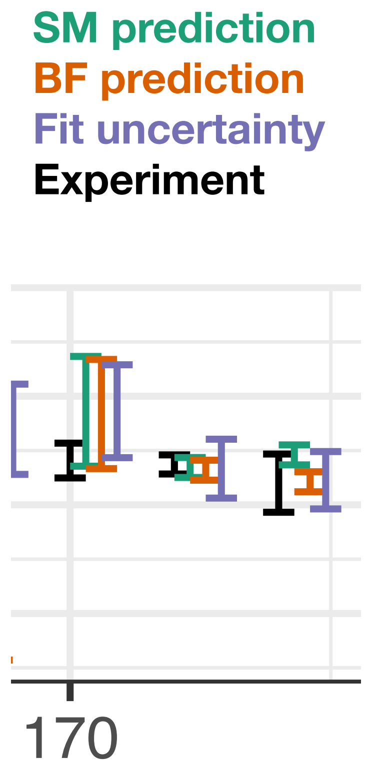

With correlation

Mostly C_7

1+		1-	
ID	δ^2	ID	δ^2
171	4.07	171	5.03
170	0.49	170	0.64
41	0.30	49	0.35
49	0.24	41	0.27
169	0.13	169	0.17

Similar picture as before

Constraints completely dominated by observable 171: $Br(B \to X_s\gamma)$. The next one is 170: $Br(B_s \to \phi\gamma)$. Correlations do not change the picture

Ranking Observables

Mostly C_9

Without correlation

5+		5-	
ID	δ^2	ID	δ^2
57	0.93	49	0.64
49	0.72	68	0.58
52	0.56	155	0.49
44	0.56	41	0.43
171	0.35	93	0.42

$P_2(B \to K^* \mu\mu)[6-8]$

$10^7 \times Br(B^0 \to K^{0*} \mu\mu)[15-19]$

$10^7 \times Br(B \to K^* \mu\mu)[16-19]$

As compared to C_7 the constraints much more balanced
→ combination
of observables is important

moving towards
the SM

5+		5-	
ID	δ^2	ID	δ^2
49	1.20	49	1.14
57	1.15	41	0.47
52	0.66	171	0.37
44	0.48	44	0.27
56	0.42	57	0.26

$P_2(B \to K^* \mu\mu)[6-8]$

$P_2(B \to K^* \mu\mu)[4-6]$

With correlation

Quite different, BR observables drop out, angular observables become more important

useful to place new results in context: example Moriond 2019

- The LHCb collaboration has a new measurement of R_K

$$R_K^{[1.1,6]} = \frac{\mathcal{B}(B \to K\mu^+\mu^-)}{\mathcal{B}(B \to Ke^+e^-)} = 0.846^{+0.060+0.016}_{-0.054-0.014}$$

- The Belle collaboration has new results for $R_{K^\star}$

$$\begin{aligned} R_{K^\star}^{[0.045,1.1]} &= 0.52^{+0.36}_{-0.26} \pm 0.05 \\ R_{K^\star}^{[1.1,6]} &= 0.96^{+0.45}_{-0.29} \pm 0.11 \\ R_{K^\star}^{[0.1,8]} &= 0.90^{+0.27}_{-0.21} \pm 0.10 \\ R_{K^\star}^{[15,19]} &= 1.18^{+0.52}_{-0.32} \pm 0.10 \\ R_{K^\star}^{[0.045,]} &= 0.94^{+0.17}_{-0.14} \pm 0.08 \end{aligned}$$

- A new combination of the new ATLAS result with previous CMS and LHCb results

$$\mathcal{B}(B_s \to \mu^+\mu^-) = 2.65^{+0.43}_{-0.39} \times 10^{-9}$$

without redoing the fit

SM prediction
BF prediction
Fit uncertainty

measurement 2019

old measurement

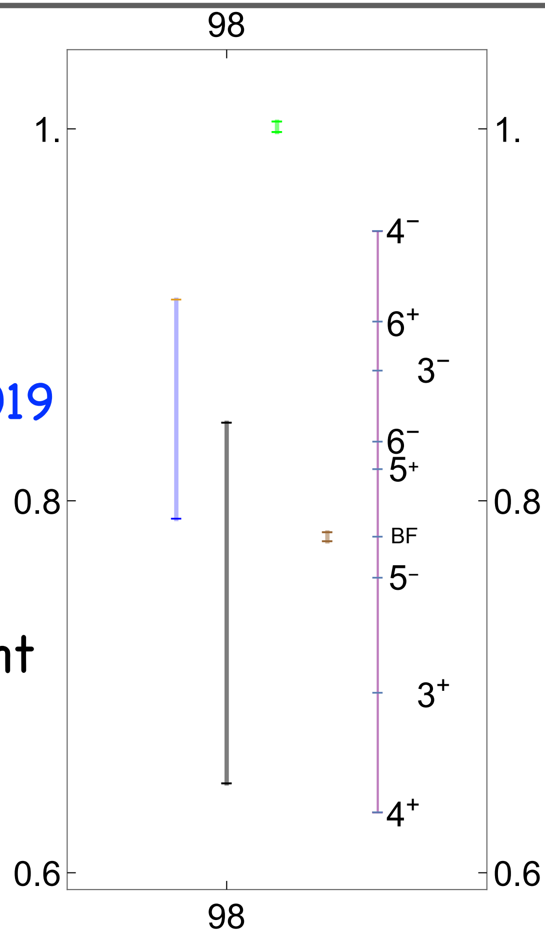

- new value of $R_K^{[1.1-6]}$ shifts BF towards SM along direction 4-
- results in a reduction in C_{10}
- R_K now completely dominates direction 4, (mostly C_{10} with a smaller admixture of C_9)

ID	$\lvert\delta^{3+}\rvert^2$	$\lvert\delta^{3-}\rvert^2$	$\lvert\delta^{4+}\rvert^2$	$\lvert\delta^{4-}\rvert^2$	$\lvert\delta^{5+}\rvert^2$	$\lvert\delta^{5-}\rvert^2$	$\lvert\delta^{6+}\rvert^2$	$\lvert\delta^{6-}\rvert^2$
98	0.75	0.85	2.30	2.90	0.14	0.05	1.40	0.28
	2.00	2.30	6.30	7.80	0.38	0.14	3.80	0.75
$\lvert\delta\rvert^2_{\max}$	1.0 (68)	0.9 (57)	2.3 (98)	2.9 (98)	0.9 (57)	0.6 (49)	1.4 (98)	2.0 (68)

without redoing the fit

SM prediction

BF prediction

Fit uncertainty

measurement 2019

old measurement

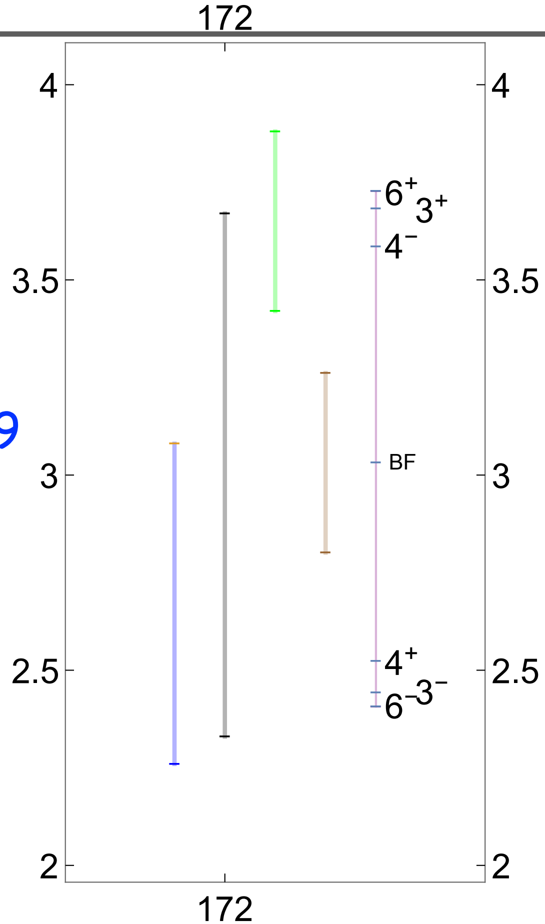

- new number $Br(B_s \to \mu^+\mu^-)$ is pushing away from **both** SM and BF
- largest impact on 6 and 3 with shifts along 6^- and 3^-.
- competing in 6 with 98, don't expect large effect on C_9
- shift along 3^- prefers a negative $C_{10'}$

ID	$\lvert\delta^{3+}\rvert^2$	$\lvert\delta^{3-}\rvert^2$	$\lvert\delta^{4+}\rvert^2$	$\lvert\delta^{4-}\rvert^2$	$\lvert\delta^{5+}\rvert^2$	$\lvert\delta^{5-}\rvert^2$	$\lvert\delta^{6+}\rvert^2$	$\lvert\delta^{6-}\rvert^2$
172	0.85 1.90	0.69 1.60	0.51 1.20	0.61 1.40	0.01 0.02	0.01 0.02	0.97 2.20	0.78 1.80
$\lvert\delta\rvert^2_{\max}$	1.0 (68)	0.9 (57)	2.3 (98)	2.9 (98)	0.9 (57)	0.6 (49)	1.4 (98)	2.0 (68)

Summary of six-d fit

- The 6d-1σ region is separated from the SM mostly along $C_{9.}$ This is the only direction where the SM point is not inside the 1σ region.
- Correlations reduce the preference for the BF over the SM for angular observables (such as P_5')
- used the Hessian to discuss fit uncertainties, lower dimensional fits and relations between parameter directions and observables
- estimate of the effect of future measurements in the global fit

For specific directions

- the most constrained direction 1 corresponds mostly to C_7 and is dominated by $B \to X_s \gamma$
- the next most constrained direction 2 ($C_{7'}$) is also dominated by one observable: low q^2 bins for P_1
- in direction 3 (mostly $C_{10'}$) the constraints accumulate from multiple observables and correlations play an important role
- direction 4 is dominated by R_K (especially after Moriond) and constrains mostly C_{10}
- direction 5 (mostly C_9) is quite complex with multiple observables providing similar constraints. We find that it is more sensitive to P_2 than to P_5', R_K, R_{K^*}

general 2HDM (FCNC) Yukawa's

with PhD student Cristian Sierra

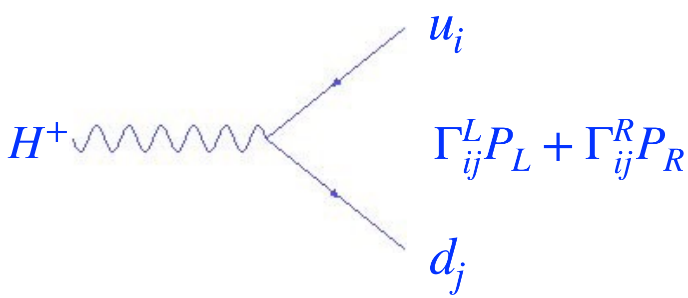

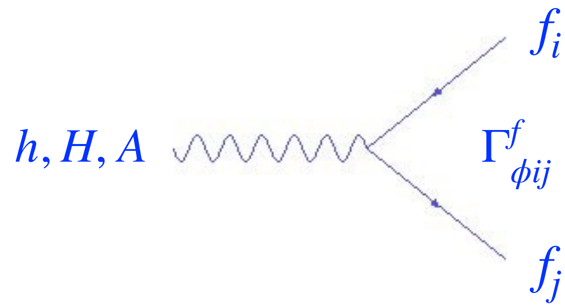

$$\Gamma^L_{ij} = \frac{\sqrt{2} m_{u_i}}{v} V_{lj} \left(Y\,\delta_{il} - \frac{f(Y)}{\sqrt{2}} \sqrt{\frac{m_{u_l}}{m_{u_i}}}\, \tilde{\chi}^u_{il} \right), \; \Gamma^R_{ij} = \frac{\sqrt{2} m_{d_l}}{v} V_{il} \left(X\,\delta_{lj} - \frac{f(X)}{\sqrt{2}} \sqrt{\frac{m_{d_j}}{m_{d_l}}}\, \tilde{\chi}^d_{lj} \right),$$

$$\Gamma^R_{\nu_i l_j} = \frac{\sqrt{2} m_{l_i}}{v} \left(Z\,\delta_{ij} - \frac{f(Z)}{\sqrt{2}} \sqrt{\frac{m_{l_j}}{m_{l_i}}}\, \tilde{\chi}^l_{ij} \right), \; \Gamma^{u,dl}_{hij} = \frac{m_{f_i}}{v} \left(\xi^f_h \delta_{ij} \mp \frac{(\xi^f_H \pm x \xi^f_h)}{\sqrt{2} f(x)} \sqrt{\frac{m_{fj}}{m_{f_i}}} \tilde{\chi}^f_{ij} \right),$$

$$\Gamma^{u,dl}_{Hij} = \frac{m_{f_i}}{v} \left(\xi^f_H \delta_{ij} \pm \frac{(\xi^f_h \mp x \xi^f_H)}{\sqrt{2} f(x)} \sqrt{\frac{m_{fj}}{m_{f_i}}} \tilde{\chi}^f_{ij} \right), \; \Gamma^f_{Aij} = -\frac{i m_{f_i}}{v} \left(X \delta_{ij} - \frac{f(X)}{\sqrt{2}} \sqrt{\frac{m_{fj}}{m_{f_i}}} \tilde{\chi}^f_{ij} \right),$$

$\chi \to 0$ recover the flavour conserving models

2HDM-III	X	Y	Z	ξ^d_h	ξ^d_H	ξ^l_h	ξ^l_H
Model I	$-\cot\beta$	$\cot\beta$	$-\cot\beta$	c_α/s_β	s_α/s_β	c_α/s_β	s_α/s_β
Model II	$\tan\beta$	$\cot\beta$	$\tan\beta$	$-s_\alpha/c_\beta$	c_α/c_β	$-s_\alpha/c_\beta$	c_α/c_β
Model Y	$\tan\beta$	$\cot\beta$	$-\cot\beta$	$-s_\alpha/c_\beta$	c_α/c_β	c_α/s_β	s_α/s_β
Model X	$-\cot\beta$	$\cot\beta$	$\tan\beta$	c_α/s_β	s_α/s_β	$-s_\alpha/c_\beta$	c_α/c_β

operators for b → s μ μ

- The model will in general produce all the operators listed before, $O_{7,9,10}$ and $O_{7',9',10'}$ in addition to scalar and pseudo scalar operators
- at tree level: $O_{S,P}$ (below) and $O_{S',P'}$ with $P_R \to P_L$

$$\mathcal{O}_S = \frac{4G_F}{\sqrt{2}} V_{tb} V_{ts}^* \frac{\alpha}{4\pi} m_b (\bar{s} P_R b)(\bar{\ell}\ell) \qquad \mathcal{O}_P = \frac{4G_F}{\sqrt{2}} V_{tb} V_{ts}^* \frac{\alpha}{4\pi} m_b (\bar{s} P_R b)(\bar{\ell}\gamma_5 \ell),$$

$$C_S^{(0)} = C_S^{(0)'} = \left(\frac{\Gamma^d_{hbs}\Gamma^l_{h\mu\mu}}{m_h^2} + \frac{\Gamma^d_{Hbs}\Gamma^l_{H\mu\mu}}{m_H^2} \right) \qquad C_P^{(0)} = -C_P^{(0)'} = \frac{\Gamma^d_{Abs}\Gamma^l_{A\mu\mu}}{m_A^2}$$

- the rest at one loop.
- We will only keep $C_{9,10}$ at one loop
  - prejudice from previous fits, $C_{9',10'}$ relatively suppressed by masses
  - use $C_{7,7'}$ as constraints ($B \to X_s \gamma$)

the 4 parameter fit

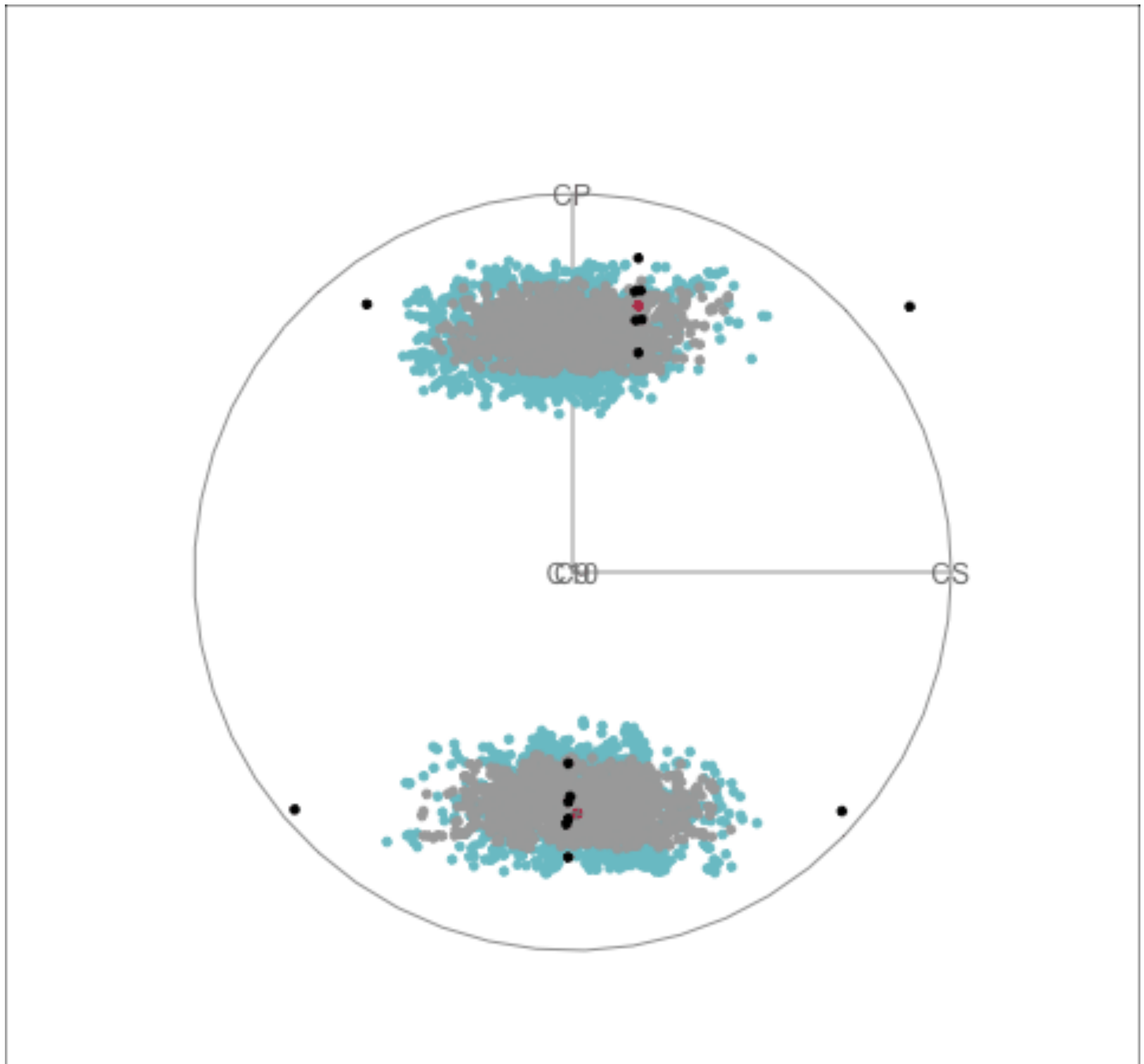

allowed region in model parameters

- would like to map the allowed (1 sigma) region (red points) to the model parameters
- equivalently the excluded (>1 sigma) region (blue points)
- usual 2d plots can't do it as inclusion (exclusion) depends on the other dimensions

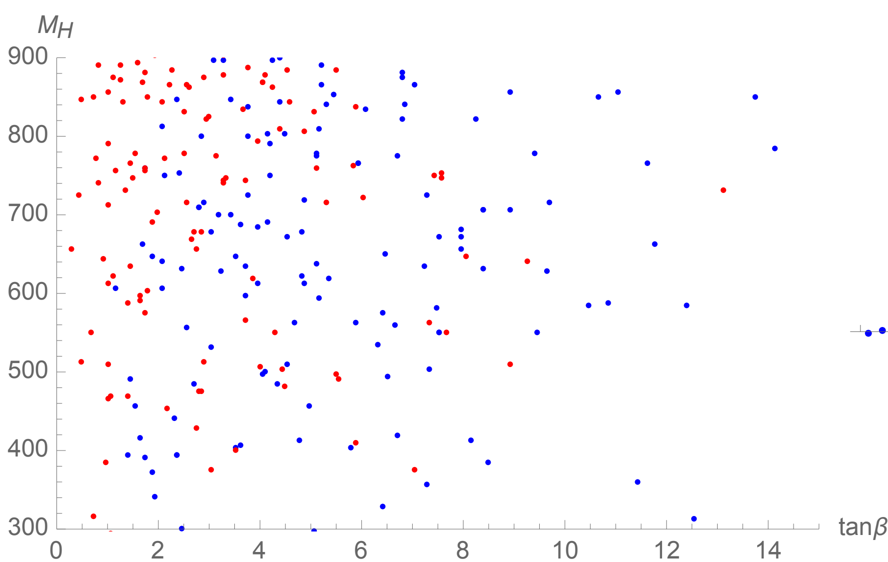

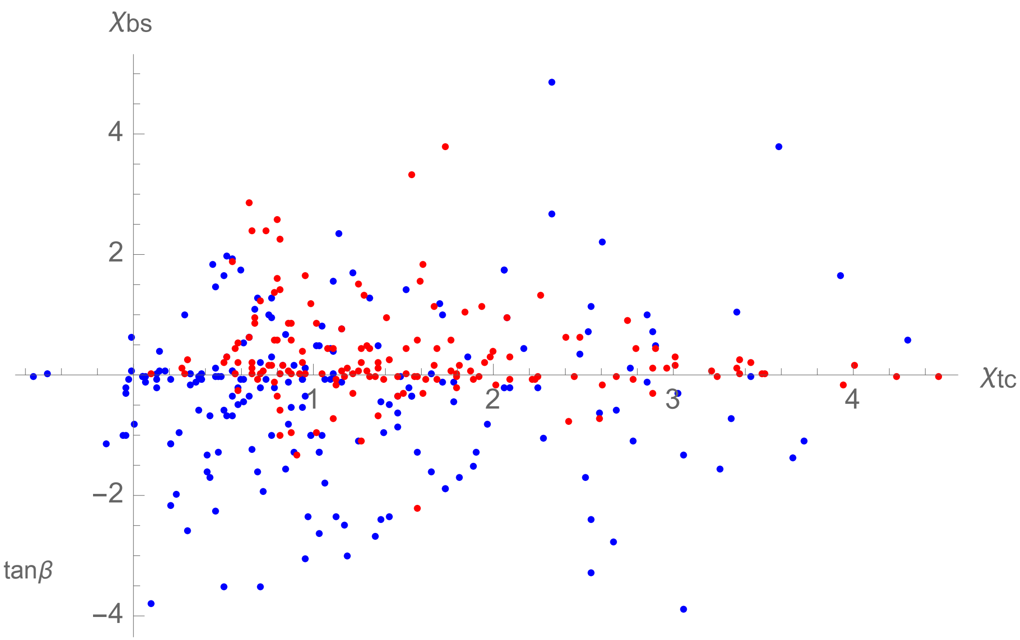

projection pursuit

- find the “most interesting” projection
- define interesting
- in this case the overlap between the allowed (1 sigma) region and the excluded (> 1 sigma) region in model parameter space
- minimise the function that parametrises this overlap as the tour moves through projections
- stop when minimum is found

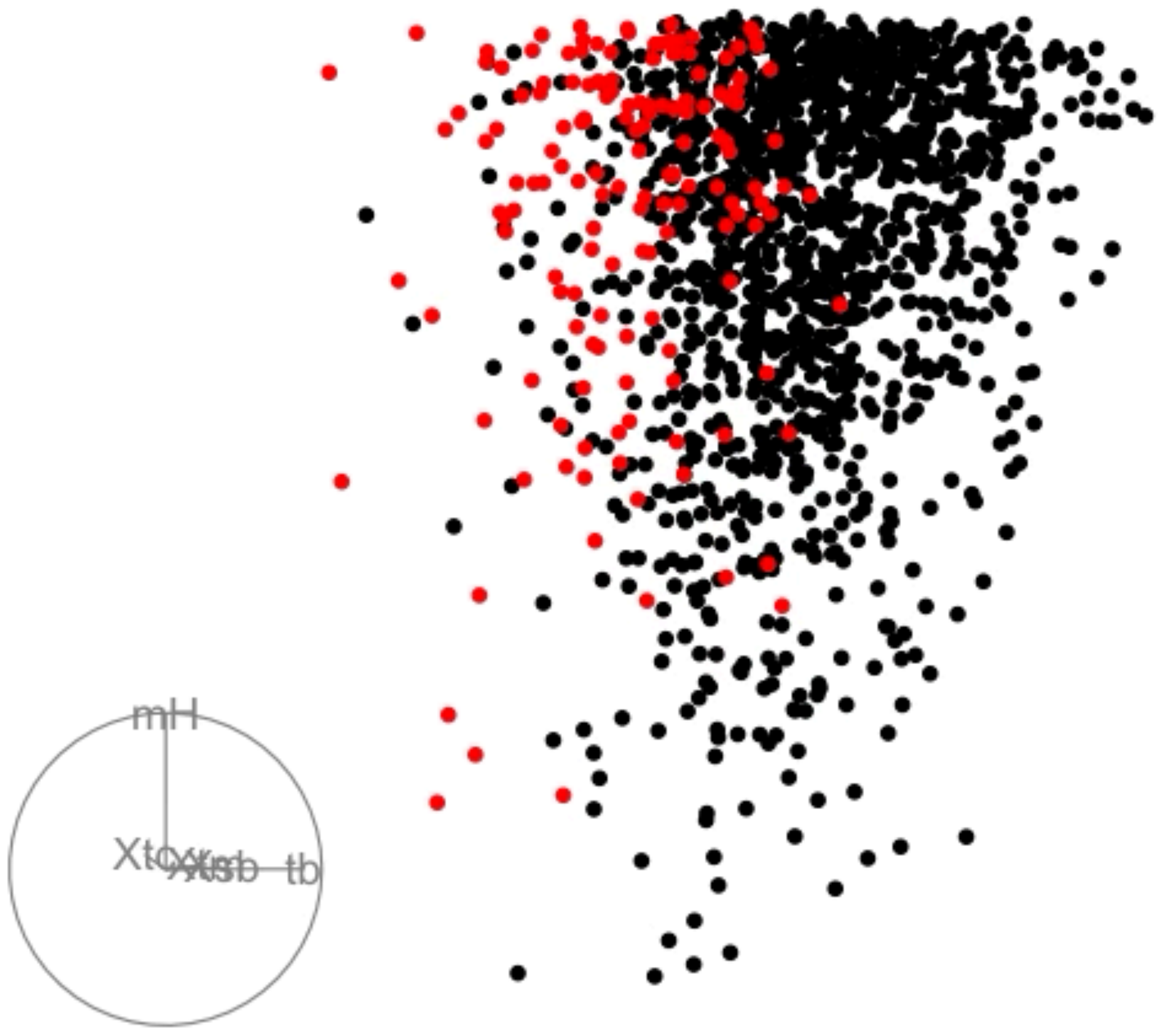

some combination consisting mostly of
$\tan\beta$ and χ_{sb} is most determining for exclusion

App developed by Ursula Laa: https://uschilaa.github.io/galahr/